Shape transitions and isotope shifts of proton and neutron distributions in the samarium isotopes

J. Jänecke and F. D. Becchetti
Department of Physics, The University of Michigan, Ann Arbor, Michigan 48109
(Received 28 December 1982)

The isotope shifts of the radii of the distributions of neutron and nucleon matter in the samarium isotopes are deduced by combining data from x-ray, muonic x-ray, and optical isotope shift measurements of charge (proton matter) radii with data for the isotope shifts of Coulomb displacement energies. The average isotope shifts from $A=144$ (spherical) to $A=154$ (deformed) are nearly the same for proton and neutron matter with $\gamma_N \approx 1.3$ or $\langle r^2 \rangle^{1/2} \propto A^{0.43}$. The neutron matter radii increase more rapidly than the proton matter radii in the region of the light transitional Sm isotopes. The transition from spherical to deformed ground states between $N=88$ and 90 is accompanied by a strong increase in the radius of the proton matter distribution ($\gamma_N \approx 1.9$), whereas the radius of the neutron-excess matter distribution remains almost constant ($\gamma_N \approx 0.0$). The data suggest strong even/odd staggering effects for both proton *and* neutron matter radii which are out of phase. The droplet model of the atomic nucleus when combined with experimental deformation parameters describes the isotope shift of the charge radii very well. The influence of zero-point vibrations in the light transitional Sm isotopes is apparent. The isotope shift of the neutron matter radii appears to be overestimated. The interacting boson model is found to describe the isotope shift of neutron matter radii satisfactorily but fails to reproduce the isotope shift of the charge radii.

[NUCLEAR STRUCTURE Deduced isotope shifts of neutron-excess, neutron, and nucleon matter radii. Interpretation of isotope shifts of proton and neutron matter radii with droplet model and interacting boson model.]

I. INTRODUCTION

Data and information on nuclear sizes and shapes provide sensitive tests for nuclear models.[1] The most direct determination of nuclear charge distributions (proton matter) comes from elastic electron scattering experiments such as the pioneering work done at Stanford.[2] However, many other experimental techniques now provide additional precise information, particularly about the isotope shifts which reflect the variation of the spatial distribution of the protons in response to the addition of neutrons. Historically, optical isotope shift measurements have played a particularly important role. The well-known Brix-Kopfermann diagram[3] demonstrated that enormous but systematic variations exist over the entire range of nuclei, with an unusually strong isotope shift for the light deformed rare-earth nuclei ($N \approx 88$). While extensive data exist[2,4–6] for nuclear charge distributions, significantly less experimental information is available for the distributions of neutron matter. It is the purpose of the present work to deduce information on the latter by combining experimental data for charge radii and Coulomb displacement energies. This procedure is based on the fact that Coulomb displacement energies depend on the distribution of both the Z protons inside the nucleus *and* the $N-Z$ excess neutrons.

The present work involving the sequence of samarium isotopes is of particular interest since it encompasses the transition from the spherical nucleus ^{144}Sm to the strongly deformed nucleus ^{154}Sm. A discontinuous transition from spherical to statically deformed ground states is known to exist[7] between ^{150}Sm and ^{152}Sm, and its influence on the distribution of both proton and neutron matter can be studied. Furthermore, contributions due to zero-point oscillations of nuclear excitation modes may also have to be considered.[8–10]

The data and information for the isotope shifts of the various radii as well as Coulomb displacement energies are presented in Secs. II–IV. The results

are discussed in Sec. V including comparisons with predictions based on the droplet model of the atomic nucleus[11] and the interacting boson model.[12]

II. ISOTOPE SHIFT COEFFICIENT γ_N OF CHARGE RADII

Direct determinations of the nuclear rms charge radii of Sm isotopes have come mostly from electron scattering experiments ($A=148$, 150, and 152, Ref. 13; $A=154$, Ref. 14). One muonic x-ray measurement has also been reported ($A=152$, Ref. 15). Most of the data are compiled in Ref. 5.

It appears, though, that considerably more precise data exist for the *isotope shift* of the charge radii, as they involve the determination of radius differences only. The techniques are more varied and include the measurement of $K\alpha$ x rays,[16–18] of muonic x rays,[19,20] and of optical transitions.[3,21–24] The results from the different types of measurements are in good agreement with one another. The differences

$$\delta\langle r^2\rangle \equiv \langle r_{N+2}{}^2\rangle - \langle r_N{}^2\rangle$$

are listed in Table I. The optical data[3,21–24] yield a quantity λ which is equal to $\delta\langle r^2\rangle$ only in first order, as it includes small corrections from terms with $\delta\langle r^4\rangle$ and $\delta\langle r^6\rangle$. A model-dependent calculation[24] yields $\delta\langle r^2\rangle \approx 1.046\lambda$, in agreement with an earlier estimate.[25] Applying this correction improves the agreement between the optical data and the other data. (Only the averaged values displayed in Table I include this correction.)

The uncertainties of the averaged values were obtained by assuming that the quoted uncertainties are statistical in nature. While this is not always the case, the consistency of the data seems to justify this procedure. Also shown in Table I are standard shifts calculated under the assumption that the rms radii increase proportional to $A^{1/3}$. Most measured isotope shifts are between even-A isotopes, but several shifts for nearest neighbors have also been determined.

Additional extensive optical isotope shift measurements for the Sm isotopes[26,27] have revealed an anomalous effect which involves certain optical transitions in only one isotopic pair. It appears that the anomaly resides in two close atomic levels in ^{154}Sm (only) which mix via higher-order perturbations. While the results from the present work make it possible to determine the off-diagonal matrix elements with an accuracy of 2–3 %, the origin of the effect (apparently neither entirely atomic nor nuclear in nature) seems to be still uncertain.

Isotope shift coefficients γ_N of the rms radii (or of other quantities such as Coulomb displacement energies) are defined by

$$\gamma_N \equiv \frac{\delta\langle r^2\rangle}{\delta\langle r^2\rangle_{\rm std}} . \tag{1}$$

The quantity γ_N describes the shift in a radius when the neutron number is changed. We will use the notation $\gamma_N(p),\gamma_N(n),\ldots,$ to describe the shift in proton, neutron, and other radii. Equation (1) can be rewritten as

$$\gamma_N = \frac{3}{2}\frac{A}{\delta N}\frac{\delta\langle r^2\rangle}{\langle r^2\rangle} = \frac{3A}{\delta N}\frac{\delta\langle r^2\rangle^{1/2}}{\langle r^2\rangle^{1/2}} . \tag{2}$$

Isotone and other shift coefficients are defined accordingly.[2,4,8]

Isotope shift coefficients γ_N for the nuclear charge radii calculated from the averaged data of Table I are included in Table III. The charge (or proton matter) distribution, like all other matter distributions discussed in this work (for protons, neutron excess, neutrons, all nucleons), are convolutions of the distributions of proton and neutron centers with the finite proton or neutron size.

III. ISOTOPE SHIFT COEFFICIENTS γ_N OF COULOMB DISPLACEMENT ENERGIES AND OF THE RADII OF NEUTRON-EXCESS MATTER DISTRIBUTION

Coulomb displacement energies between isobaric analog states depend on the distribution of the proton core *and* that of the neutron excess. The direct Coulomb displacement energy which comprises typically 95% of the total can be written as[28]

$$\Delta E_C^{\rm dir} = \frac{e}{2T}\int \rho_{\rm exc}(\vec{r})V_{\rm core}(\vec{r})d^3\vec{r} . \tag{3}$$

Here, $\rho_{\rm exc}(\vec{r})$ is the matter distribution of the neutron excess, and $V_{\rm core}(\vec{r})$ is the electrostatic potential of the proton core. Equation (3) can also be expressed[8,29] in a form which is completely symmetric in its dependence on the two distributions,

$$\Delta E_C^{\rm dir} = 4\pi\sum_{\lambda\mu}\int_0^\infty r^{-(2\lambda+2)}M_{\rm exc}(E\lambda\mu,r)M_{\rm core}(E\lambda\mu,r)dr , \tag{4}$$

where

$$M_{\rm core}(E\lambda\mu,r') = e\int_{4\pi}\int_0^{r'} r^\lambda Y_{\lambda\mu}(\theta,\phi)\rho_{\rm core}(\vec{r})r^2dr\,d\Omega \tag{5}$$

and

$$M_{\rm exc}(E\lambda\mu,r')=\frac{e}{2T}\int_{4\pi}\int_0^{r'} r^{\lambda}Y_{\lambda\mu}(\theta,\phi)\rho_{\rm exc}(\vec{r})r^2dr\,d\Omega \tag{6}$$

are generalized electric multipole operators. These operators reduce to the ordinary electric multipole operator if the radial integrations are carried out to infinity.

It follows from the above equation that there exists a direct relationship between the isotope shifts of Coulomb displacement energies, charge radii, and neutron-excess matter radii,[30]

$$-\gamma_N(\Delta E_C)\approx\tfrac{1}{2}(\gamma_N(p)+\gamma_N(n-\text{exc}))\ . \tag{7}$$

This equation is approximate to the extent that lowest order terms are sufficient to describe the variations with neutron number. Probably more important, it also assumes that the numerous small contributions to the Coulomb displacement energy from exchange, the electromagnetic spin-orbit effect, etc.,[28,31] will not seriously affect the isotope-shift relation based on the *direct* Coulomb displacement energy term.

The isotope shifts $\delta\Delta E_C$ and $\delta(\Delta E_C)^2$ derived from recently determined Q values[32] of (^{3}He,t) charge-exchange reactions on all stable Sm isotopes are shown in Table II. Also shown are the calculated values which assume an $A^{1/3}$ dependence. The isotope shift coefficients $\gamma_N(\Delta E_C)$ obtained from these values are included in Table III.

The isotope shift coefficients $\gamma_N(p)$ of the protons and $\gamma_N(\Delta E_C)$ of the Coulomb displacement energies have been used with Eq. (7) to calculate the isotope

TABLE I. Isotope shift $\delta\langle r^2\rangle$ for the charge (= proton matter) radii of the Sm isotopes. O is the optical isotope shift; X is the $K\alpha$ x-ray isotope shift; M is the muonic x-ray isotope shift.

A	$\delta\langle r^2\rangle_p$ (10^{-3} fm^2)									
	O[a]	X[b]	X[c]	O[d]	M[e]	M[f]	O[g]	O[h]	Average[i]	Std[j]
144–145										113.5
145–146										113.2
146–147										113.1
147–148			171±10	154±14			152±8	149±5	159±4	112.9
148–149			80±8	81±7			92±5	91±3	93±3	112.8
149–150			224±10						224±10	112.7
150–151				~178					~186	112.6
151–152										112.6
152–153										112.5
153–154										112.3
144–148	582±123	503±88		486±25		532±21	517±27	509±18	529±11	452.7
144–146										226.7
146–148										226.0
148–150	332±72	372±54	303±10	294±15		315±19	303±16	297±11	310±6	225.5
150–152	489±104	400±58	411±12	409±24	437±4	432±14	423±22	413±15	434±4	225.2
152–154	261±54		221±13	215±16		250±14	230±12	227±8	236±5	224.8
144–154						1529±35	1463±40	1445±33	1523±21	1128.2

[a]References 3 and 21.
[b]Reference 16.
[c]References 17 and 18.
[d]Reference 22.
[e]Reference 19.
[f]Reference 20.
[g]Reference 23.
[h]Reference 24.
[i]Values from optical isotope shift measurements have been increased by 4.6% (see text).
[j]Shift assuming an $A^{1/3}$ dependence for $\langle r^2\rangle^{1/2}$, thus $\delta\langle r^2\rangle_{\rm std}=\langle r_<{}^2\rangle((A_>/A_<)^{2/3}-1)$.

TABLE II. Isotope shifts $\delta\Delta E_C$ and $\delta(\Delta E_C)^2$ for Coulomb displacement energies and $\delta\langle r^2\rangle$ for neutron matter radii of the Sm isotopes.

	$\delta\Delta E_C$ (keV)	$\delta(\Delta E_C)^2$ (MeV^2)		$\delta\langle r^2\rangle_n$ (10^{-3} fm^2)	
A	a	a	Std[b]	c	Std[b]
144–145	−73±15	−2.34±0.48	1.191		121.6
145–146	(−52)	(−1.66)	1.176		121.5
146–147	(−61)	(−1.94)	1.158		121.4
147–148	−33±13	−1.05±0.40	1.141	122±40	121.3
148–149	−77±13	−2.44±0.40	1.129	236±69	121.2
149–150	−31±13	−0.98±0.40	1.114	127±63	121.2
150–151	−36±17	−1.13±0.55	1.099	∼135	121.1
151–152	−25±17	−0.79±0.55	1.089		121.0
152–153	(−42)	(−1.32)	1.075		120.8
153–154	(−36)	(−1.13)	1.062		120.6
144–148	−219±13	−6.99±0.41	4.666	693±107	485.8
144–146	(−125)	(−4.00)	2.367		243.1
146–148	(−94)	(−2.99)	2.300		242.7
148–150	−108±13	−3.41±040	2.243	363±36	242.4
150–152	−61±13	−1.92±0.40	2.188	247±96	242.1
152–154	−78±13	−2.44±0.40	2.137	273±40	241.4
144–154	−466±13	−14.76±0.40	11.235	1602±40	1211.8

[a]Reference 32; values based on estimated ΔE_C are given in parentheses.
[b]Shift assuming an $A^{1/3}$ dependence for ΔE_C, thus $\delta(\Delta E_C)_{\rm std}{}^2=(\Delta E_{C<})^2((A_> /A_<)^{2/3}-1)$.
[c]This work.

shift coefficient $\gamma_N(n-\text{exc})$ of the neutron excess. The results are included in Table III.

IV. ISOTOPE SHIFT COEFFICIENTS γ_N OF THE RADII OF NEUTRON AND NUCLEON MATTER DISTRIBUTIONS

The isotope shift coefficient $\gamma_N(n)$ of the neutrons is related to that of the neutron core ($N\leq 62$) and that of the neutron excess ($N>62$) according to

$$\gamma_N(n)=\frac{Z}{N}\gamma_N(n-\text{core})+\frac{N-Z}{N}\gamma_N(n-\text{exc})\ . \tag{8}$$

However, $\gamma_N(n-\text{core})$ is not known, and Eq. (8) therefore has to be approximated by

$$\gamma_N(n)\approx x\gamma_N(p)+y\gamma_N(n-\text{exc}) \tag{9}$$

with $x+y=1$. Here, the proton core consists of all 62 protons. Three cases are considered: (i) $x=Z/N$, (ii) $x=50/N$, and (iii) $x=0$. Cases (i) and (iii) are limiting cases[33] implying that the n core has an isotope shift equal to that of the p core or the n excess, respectively. The former assumption is presumably more realistic.[33] The isotope shift coefficients $\gamma_N(n)$ of Table III were obtained with $x=50/N$, but with uncertainties increased to include the values for $x=Z/N$ and their uncertainties. This procedure was chosen since the major fraction of the excess neutrons ($N>62$) consists of neutrons in the major shell $50<N\leq 82$. The shifts $\delta\langle r^2\rangle$ for the neutrons (Table II) are calculated from the above coefficients $\gamma_N(n)$ and the standard shifts.

The isotope shift coefficients $\gamma_N(\text{nucl})$ for the matter distribution of all nucleons are obtained from

$$\gamma_N(\text{nucl})=\frac{Z}{A}\gamma_N(p)+\frac{N}{A}\gamma_N(n) \tag{10}$$

and are included in Table III.

V. DISCUSSION

A. General considerations

The isotope shift coefficients γ_N between even-A isotopes (Table III) are displayed in Figs. 1 and 2 as a function of mass number A. The data points are plotted for the lower value of A. Figure 1 displays

TABLE III. Isotope shift coefficients γ_N for the Sm isotopes.

A	Proton matter[a]	Coulomb energies[b]	Neutron excess matter[c]	Neutron matter[c]	Nucleon matter[c]
144–145		−1.97±0.40			
145–146		(−1.41)			
146–147		(−1.68)			
147–148	1.41±0.04	−0.92±0.35	0.43±0.70	1.01±0.33	1.18±0.19
148–149	0.82±0.03	−2.16±0.36	3.50±0.71	1.94±0.57	1.48±0.33
149–150	1.99±0.09	−0.88±0.36	−0.23±0.72	1.05±0.52	1.44±0.31
150–151	~1.65	−1.03±0.50	~0.40	~1.11	~1.34
151–152		−0.72±0.50			
152–153		(−1.22)			
153–154		(−1.06)			
144–148	1.17±0.03	−1.50±0.09	1.83±0.18	1.43±0.22	1.32±0.13
144–146					
146–148					
148–150	1.37±0.03	−1.52±0.18	1.67±0.36	1.50±0.15	1.45±0.09
150–152	1.93±0.02	−0.88±0.18	−0.17±0.37	1.02±0.40	1.40±0.23
152–154	1.05±0.03	−1.14±0.19	1.23±0.38	1.13±0.17	1.10±0.10
144–154	1.35±0.02	−1.31±0.04	1.28±0.07	1.32±0.03	1.33±0.02

[a]References 3, 16–24.
[b]Reference 32.
[c]Deduced; this work.

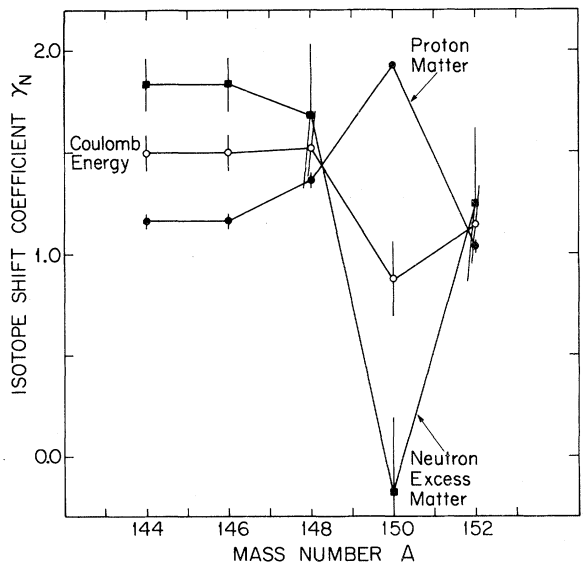

FIG. 1. Isotope shift coefficients γ_N of proton matter (charge) and neutron-excess matter radii and of Coulomb displacement energies (absolute values) of the even-A Sm isotopes. The data are plotted for the lower value of A, and the shifts between $A=144$ and 148 are displayed at $A=144$ *and* 146.

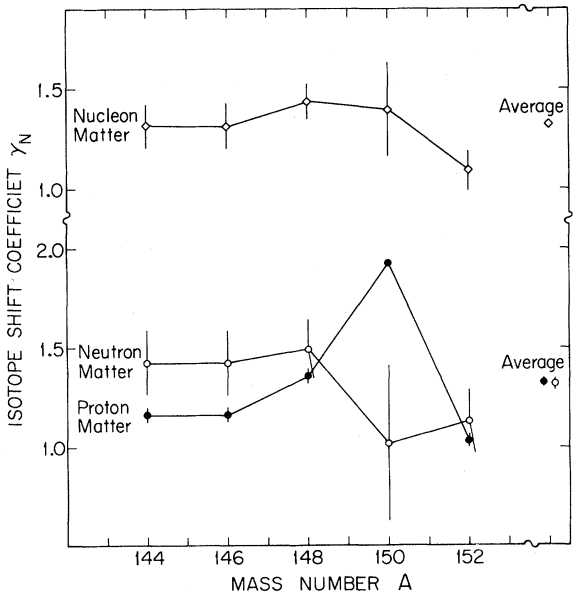

FIG. 2. Isotope shift coefficients γ_N of proton, neutron, and nucleon matter radii of the even-A Sm isotopes. The data are plotted for the lower value of A, and the shifts between $A=144$ and 148 are displayed at $A=144$ *and* 146.

γ_N for protons, neutron excess, and the Coulomb displacement energies (absolute values). Figure 2 displays γ_N for protons, neutrons, and all nucleons. As mentioned previously, nucleon sizes are included in all the distributions. Also, the γ_N for neutron excess and for all neutrons are not the results of a direct measurement but are deduced from Eq. (7) or (9), respectively. The shifts between $A=144$ and 148 are plotted at both $A=144$ and 146 to facilitate the discussion.

The neutron-excess radii increase at a substantially higher rate than the proton radii in the light transitional Sm nuclei. This behavior is dramatically reversed between $A=150$ and 152 where the neutron-excess radii remain practically constant, $\gamma_N \approx 0$, while proton radii increase at an exceptionally high rate with $\gamma_N \approx 1.9$. The rates of increase beyond $A=152$ are again similar to those in the lighter Sm isotopes.

The isotope shift coefficient γ_N for all neutrons, Fig. 2, does not display the strong decrease between $A=150$ and 152. The core neutrons are apparently influenced less by the effect which causes the sudden change for the protons and the neutron excess. The isotope shift coefficients γ_N for all nucleons remain practically the same over the entire range, and there is no anomaly at $A=150-152$. Another interesting observation is apparent from the figures: Whereas the individual shifts for the protons and neutrons differ greatly, their average isotope shift coefficients γ_N from $A=144$ to 154 are essentially identical.

A simple qualitative explanation of the observed phenomena in the Sm isotopes is provided by considering the dependence of deformation on neutron number. The semimagic nucleus ^{144}Sm is spherical, while ^{154}Sm is strongly deformed.[34–36] A discontinuous transition from spherical to statically deformed ground states is known to take place between $A=150$ and 152.[7] The coexistence between spherical and deformed shapes manifests itself[34] by strong two-neutron stripping reactions from the spherical ground states with $N=88$ to spherical excited states with $N=90$, and by strong two-neutron pickup reactions from deformed ground states with $N=90$ to deformed excited states with $N=88$.

The addition of neutron pairs to the spherical nucleus ^{144}Sm increases the neutron radii more rapidly than the proton radii. This appears to continue at about the same rate with the addition of up to three neutron pairs. Whereas the ground states of the even-A nuclei from ^{144}Sm to ^{150}Sm are believed to have no static deformation ($\langle\beta\rangle=0$), measurements of electromagnetic $E2$ transition rates[35] show that dynamic vibrations lead to $\langle\beta^2\rangle\neq 0$. These may be viewed microscopically as zero-point motions of collective two-particle/two-hole excitation, which give rise to long-range ground state correlations.[9,10] Root-mean-square radii (as well as Coulomb energies) are affected by both, $\langle\beta\rangle$ *and* $\langle\beta^2\rangle^{1/2}$, and at least part of the increase of the proton, and particularly the neutron radii from $A=144$ to 150, is likely the result of dynamic vibrations.

The addition of the fourth neutron pair leads to a statically deformed[34] collective ground state at $N=90$. As a consequence, the effective neutron-proton interaction seems to cause a sudden increase in the radius of the proton distribution compensating for the earlier lag, whereas the neutron-excess radius remains practically constant. Strong collectivity probably also accounts for nearly equal average isotope shift coefficients over the range $A=144-154$.

An exceptionally large isotope shift from $N=88$ to 90 of the nuclear charge radii has been observed not only for Sm but also for Nd and Dy.[18,22] Furthermore, the experimental charge deformation parameters[35,36] β_2 show a strong increase from $N=88$ to 90 for Nd, Sm, Gd, and Dy (see also Ref. 37). It thus appears likely that the effect described in this work is present in all these nuclei.

B. Odd-even staggering

The data of Tables I and II show very pronounced staggering between odd-N and even-N isotopes for the radii of both protons and neutrons. The addition of one unpaired neutron increases the neutron radii significantly more than the average, and the proton radii accordingly much less than the average. The addition of a second neutron, which leads to the formation of a neutron pair, has the opposite effect. The radii of all nucleons, on the other hand, increase at the "normal" average rate in both instances. The isotope shifts of the Coulomb displacement energies seem to display a weak odd-even staggering over the entire range of the Sm isotopes, suggesting an increased influence of unpaired excess neutrons.

Odd-even staggering of nuclear charge radii has been observed in numerous instances and theoretical attempts have been made to interpret this phenomenon (see, e.g., Refs. 1, 38, and 39). Pairing correlations between neutrons have been considered,[38] including the dependence on angular momentum as well as the Pauli blocking effect initiated by an odd neutron. In another approach, deformations associated with zero-point vibrations, $\langle\beta^2\rangle$, and the blocking of ground state correlations by an odd neutron are used to explain odd-even staggering.[39] It appears, though, that a generally accepted explanation of odd-even staggering in the isotope shift of proton (charge) and neutron distributions does not yet exist. The results from the

present work suggest that contributions from isovector multipole core polarization may play an important role.

C. Droplet-model predictions including deformations

The liquid-droplet model of the atomic nucleus[11,40] can be used to calculate mean square radii of proton and neutron matter from the expression

$$\langle r^2\rangle=\langle r^2\rangle_u+\langle r^2\rangle_r+\langle r^2\rangle_d\ . \tag{11}$$

Here,

$$\langle r^2\rangle_u=\tfrac{3}{5}R^2(1+f_1(\alpha_2,\alpha_4)) \tag{12}$$

is the dominant contribution resulting from the size of a distribution of uniform density and radius R. The spherical droplet-model radius R for protons and neutrons can be taken from Ref. 11, and $f_1(\alpha_2,\alpha_4)$ is a shape correction. The redistribution term

$$\langle r^2\rangle_r=\tfrac{3}{5}R^2\tfrac{4}{35}C'(1+f_2(\alpha_2,\alpha_2)) \tag{13}$$

with shape correction $f_2(\alpha_2,\alpha_4)$ accounts for the central depression in the proton and neutron distributions. Diffuseness, finally, is included (from a folding procedure) by

$$\langle r^2\rangle_d=3\sigma^2\ , \tag{14}$$

with $\sigma=0.95$ fm. The shape correction functions are

$$f_1(\alpha_2,\alpha_4)=\alpha_2^2+\tfrac{10}{21}\alpha_2^3-\tfrac{27}{35}\alpha_2^4+\tfrac{10}{7}\alpha_2^2\alpha_4+\tfrac{5}{9}\alpha_4^2\ , \tag{15}$$

$$f_2(\alpha_2,\alpha_4)=\tfrac{14}{5}\alpha_2^2+\tfrac{28}{15}\alpha_2^3-\tfrac{29}{5}\alpha_2^4+\tfrac{116}{15}\alpha_2^2\alpha_4+\tfrac{70}{27}\alpha_4^2\ , \tag{16}$$

with

$$\alpha_L=\left[\frac{2L+1}{4\pi}\right]^{1/2}\beta_L\ . \tag{17}$$

Here, β_2 and β_4 are quadrupole and hexadecapole deformation parameters which can be taken from calculations or from experiment. Additional quantities needed for the calculation are

$$C'=\frac{1}{2}\left[\frac{9}{2K}\pm\frac{1}{4J}\right]\frac{e^2Z}{r_0A^{1/3}}\ , \tag{18}$$

where K and J are compressibility and symmetry parameters, respectively. The two signs are for protons and neutrons and Eq. (18) yields

$$\begin{aligned}C'&=0.0156ZA^{-1/3}\text{ for protons,}\\ C'&=0.0073ZA^{-1/3}\text{ for neutrons.}\end{aligned} \tag{19}$$

The comparison between experimental and calculated values is displayed in Figs. 3 and 4. Figure 3 shows the differences between the mean-square radii of the even-A isotopes; Fig. 4 shows the mean-square radii directly. The experimental values are shown as filled circles connected by solid lines. The experimental mean-square values of Fig. 4 have been arbitrarily normalized at $N=82$ to the droplet-model predictions. Also shown in Fig. 4 are absolute experimental mean-square charge radii[13–15] (filled squares) which are significantly less precise, but confirm the normalization used for the relative charge radii.

Values obtained assuming $\gamma_N\equiv1$ are included in Fig. 3 as dotted lines. Several droplet-model predictions (LDM) are included in the figures for both protons and neutrons. They are displayed as dashed lines, including results for $\beta_2=\beta_4=0$. Other LDM curves are obtained using deformation parameters β_2 and β_4 calculated from a simple semiempirical

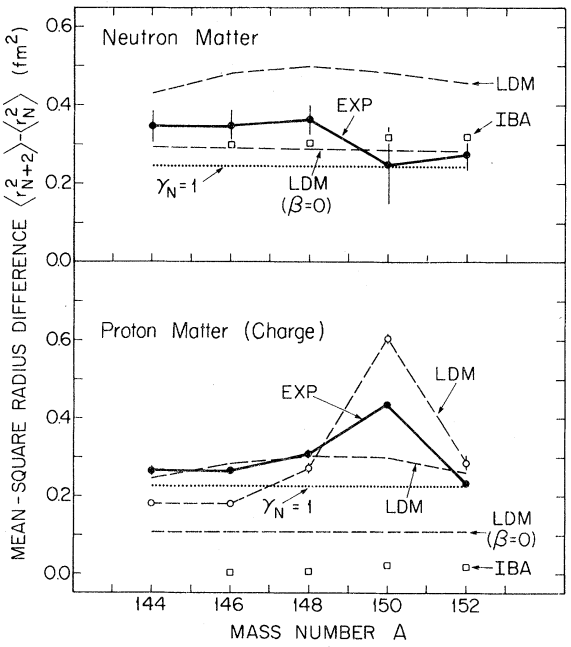

FIG. 3. Mean-square radius differences $\langle r_{N+2}{}^2\rangle-\langle r_N{}^2\rangle$ of proton and neutron matter of the even-A Sm isotopes. Filled circles and solid lines: experimental; dashed lines: liquid droplet model with $\beta=0$, $\beta=$ calculated, and $\beta=$ experimental (open circles); open squares: interacting boson model; dotted line: $\langle r^2\rangle\propto A^{2/3}$ ($\gamma_N\equiv1$).

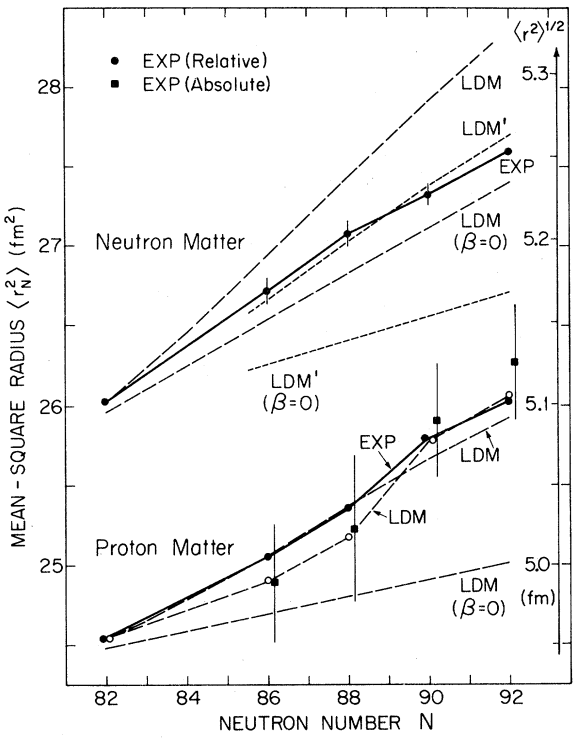

FIG. 4. Mean-square radii $\langle r_N^2 \rangle$ of proton and neutron matter of the even-N Sm isotopes. Filled circles and solid lines: experimental, normalized at $N=82$; filled squares: experimental (absolute); dashed lines: liquid droplet model with $\beta=0$, $\beta=$ calculated, and $\beta=$ experimental (open circles); narrow-dashed lines: liquid droplet model (neutron matter only) with $\beta=0$ and $\beta=$ calculated (but with artificially reduced isotope shift of the neutron sharp radius R; see text).

parametrization[37] of the experimental charge deformation parameters as well as (for protons only; open circles connected by dashed lines) for the *experimental* charge deformation parameters β_2 and β_4.

Both figures show basic agreement between the LDM predictions and the experimental values for the radii of the charge distribution. In particular, the relative values for the mean-square radii of the spherical ^{144}Sm and the statically deformed ^{152,154}Sm are in excellent agreement. The LDM predictions using experimental deformation parameters for the vibrational nuclei ^{148,150}Sm are slightly lower than the experimental values. This deviation can easily be accounted for by a slight increase of the surface diffuseness σ (see Fig. 3 of Ref. 40).

Disagreement appears to exist between the LDM predictions and the experimental values for the neutron radii. The LDM predictions are too high unless the deformation of the neutron matter is significantly less (50%) than that of the proton matter (charge). This is unlikely. In fact, recent experiments[41,42,32] suggest

$$\langle \beta^2(n) \rangle^{1/2} > \langle \beta^2(p) \rangle^{1/2}$$

for ^{148,150}Sm and $\beta(n) < \beta(p)$ for ^{152,154}Sm. (Ratios deviate from unity by about 5% to 20%.)

The isotope shifts of the neutron radii deduced in this work are not from a direct measurement. Equation (7) is the basic relationship between the isotope shifts of proton and neutron-excess matter and that of Coulomb displacement energies. It is valid only for the direct part of the Coulomb displacement energies; exchange terms, the electromagnetic spin-orbit interaction, or other small terms may contribute if their dependence on N is significantly different from that for the direct term. Their influence for the sequence of Sm isotopes, however, is not judged important because of the collective nature of the wave function. Moreover, the essentially equal isotope shifts deduced for protons and neutrons over the entire range $A=144-154$ are taken as an indication of the validity of the procedures.

The narrow dashed lines labeled LDM' for the neutron radii in Fig. 4 are obtained with radii R which were *artificially* reduced (smaller isotope shift). Deformation parameters β_2 and β_4 equal to zero and from the semiempirical parametrization were again used for the shape corrections. The assumptions yield good agreement with the data and with recent results concerning the differences between the deformations of the neutron and proton distributions.[32,41,42]

D. Interacting boson model predictions

The interacting boson model (IBA) (Ref. 12) has been used extensively[43] to describe spectra and other properties of the Sm isotopes. It includes (Fig. 13 in Ref. 43) a comparison between calculated and experimental differences of mean-square charge radii. The agreement is generally good, but the calculations do not reproduce the sharp increase from $N=88$ to 90.

The version of the interacting boson model which treats protons and neutrons separately (IBA2) has been used in the present work to describe the isotope shifts of both proton and neutron radii. The mean-square radii for both protons and neutrons can be written as[44]

$$\langle r^2 \rangle = \langle r^2 \rangle_{\text{core}} + \beta n^d + \gamma(n^s + n^d) \tag{20}$$

(superscripts π or ν on all quantities have been dropped). Here, n^s and n^d are the number of (diproton or dineutron) bosons; $N=n^s+n^d$ is the total number of bosons of each kind; and β and γ are

parameters of the IBA2 Hamiltonian (unrelated to the previous deformation parameters). The difference of the mean-square radii is obtained from Eq. (20),

$$\langle r_{N+2}{}^2\rangle - \langle r_N{}^2\rangle = \beta(n_{N+2}^d - n_N^d) + \gamma \quad (21)$$

(with superscripts ν) for the neutrons, and

$$\langle r_{N+2}{}^2\rangle - \langle r_N{}^2\rangle = \beta(n_{N+2}^d - n_N^d) + 0 \quad (22)$$

(with superscripts π) for the protons. The quantity γ^π ($\neq 0$) does not enter into Eq. (22) because the number of proton bosons ($\frac{1}{2}Z = 31$) is constant. Values of $\gamma^\nu \approx 0.3$ and $\beta^\nu \approx \beta^\pi \approx 0.02$ are typical,[44] but small variations are possible. The differences in the number of proton (neutron) d bosons have been calculated.[44] They are in the range 0.2—1.0 for both proton and neutron bosons, increasing with neutron number. The results are displayed in Fig. 3 as open squares. Whereas the experimental neutron mean-square radius differences are well reproduced, the calculations fail to describe the observed proton mean-square radii.

Two problems can account for this behavior. The ν-boson-π-boson interaction resides in the quadrupole-quadrupole interaction but individually conserves the number of neutron and proton bosons. Hence,

$$\langle r_{N+2}{}^2\rangle - \langle r_N{}^2\rangle \approx 0$$

is predicted for the protons. Perhaps more importantly, the step from Eq. (20) to (21) assumes that $\langle r^2\rangle_{\text{core}}$ remains constant for both neutrons *and* protons when neutron bosons are added. However, core polarization is believed (e.g., Ref. 39) to play a major role in the interpretation of isotope shifts.

VI. SUMMARY AND CONCLUSIONS

The radii of the excess neutrons increase more rapidly than the proton radii in the light Sm isotopes. This appears to be the result of neutron dynamic zero-point vibrations. When the phase transition takes place at $N = 88$—90 the neutron-excess radius remains essentially constant, whereas the proton radius increases at an exceptionally high rate and compensates for the earlier lag. The average isotope shifts for all neutrons and protons from the spherical ^{144}Sm to the statically deformed ^{154}Sm are about equal, as is expected from the strong collectivity.

Strong odd-even staggering is suggested by the data whereby the addition of a single odd neutron increases the neutron radii much more than the proton radii. The addition of a second neutron to form a pair has the opposite effect. A comprehensive explanation of odd-even staggering does not seem to exist.

The droplet model of the atomic nucleus[11,40] combined with experimental deformation parameters describes the isotope shifts of proton radii very well, but appears to overestimate that of the neutron radii. The interacting boson model (IBA2) describes neutron radii quite well but fails for proton radii. This may indicate the presence of strong core polarization effects.

ACKNOWLEDGMENTS

Discussions with D. L. Clark, K. T. Hecht, W. D. Myers, and O. Scholten are highly appreciated. Particular thanks are due to O. Scholten for the IBA calculations and to D. L. Clark for permission to present the data of Ref. 24 prior to publication. This work was supported in part by the National Science Foundation, Grant No. PHY78-07754.

[1]R. C. Barrett and D. F. Jackson, *Nuclear Sizes and Structure* (Clarendon, Oxford, 1977).

[2]H. R. Collard and R. Hofstadter, *Nuclear Radii,* in Landolt-Börnstein: Numerical Data and Functional Relationships in Science and Technology (Springer, Berlin, 1967), New Series, Group I, Vol. 2, p. 21.

[3]F. Brix and H. Kopfermann, Rev. Mod. Phys. 30, 517 (1958); H. Kopfermann, *Nuclear Moments* (Academic, New York, 1958).

[4]L. R. B. Elton, *Nuclear Radii,* in Landolt-Börnstein: Numerical Data and Functional Relationships in Science and Technology (Springer, Berlin, 1967), New Series, Group I, Vol. 2, p. 1.

[5]C. W. de Jager, H. de Vries, and C. de Vries, At. Data Nucl. Data Tables 14, 479 (1974).

[6]R. Engfer, H. Schneuwly, J. L. Vuilleumier, H. K. Walter, and A. Zehnder, At. Data Nucl. Data Tables 14, 509 (1974).

[7]G. Scharff-Goldhaber and J. Weneser, Phys. Rev. 98, 212 (1955).

[8]J. Jänecke, in *Atomic Masses and Fundamental Constants* 4, edited by J. H. Sanders and A. H. Wapstra (Plenum, London/New York, 1972), p. 221.

[9]S. Ullrich and E. W. Otten, Nucl. Phys. A248, 173 (1975).

[10]P. G. Reinhard and D. Drechsel, Z. Phys. A 290, 85 (1979).

[11]W. D. Myers, *Droplet Model of Atomic Nuclei* (EFI/Plenum, New York, 1977).

[12]A. Arima and F. Iachello, Phys. Rev. Lett. 35, 1069

(1975).
[13]L. S. Cardman, D. Kalinsky, J. R. Legg, R. Yen, and C. K. Bockelman, Nucl. Phys. A216, 285 (1973).
[14]J. Heisenberg, private communication; quoted in Ref. 5.
[15]D. Hitlin, S. Bernow, S. Devons, I. Duerdoth, J. W. Kast, E. R. Macagno, J. Rainwater, C. S. Wu, and R. C. Barret, Phys. Rev. C 1, 1184 (1970).
[16]O. I. Sumbaev, E. V. Petrovitch, V. S. Sykov, A. S. Rylnikov, and A. I. Grushko, Yad. Fiz. 5, 544 (1967) [Sov. J. Nucl. Phys. 5, 387 (1967)].
[17]P. L. Lee and F. Boehm, Phys. Lett. 35B, 33 (1971); Phys. Rev. C 8, 819 (1973).
[18]F. Boehm and P. L. Lee, At. Data Nucl. Data Tables 14, 605 (1974).
[19]Y. Yamasaki, E. B. Shera, M. V. Hoehn, and R. M. Steffen, Phys. Rev. C 18, 1474 (1978).
[20]R. J. Powers, P. Barreau, B. Bihoreau, J. Miller, J. Morgenstern, J. Piccard, and L. Roussel, Nucl. Phys. A316, 295 (1979).
[21]A. S. Meligdy, S. Tadros, and M. A. El-Wahab, Nucl. Phys. 16, 99 (1960); E. E. Fradkin, Zh. Eksp. Teor. Fiz. 42, 787 (1962) [Sov. Phys.—JETP 15, 550 (1962)]; F. A. Babushkin, *ibid.* 44, 1661 (1963) [*ibid.* 17, 1118 (1963)].
[22]K. Heilig and A. Steudel, At. Data Nucl. Data Tables 14, 613 (1974).
[23]H. Brand, B. Seibert, and A. Steudel, Z. Phys. A 296, 281 (1980).
[24]D. L. Clark, Ph.D. thesis, University of Minnesota, 1977 (unpublished); D. L. Clark and G. W. Greenlees (unpublished).
[25]E. C. Seltzer, Phys. Rev. 188, 1916 (1969).
[26]J. A. R. Griffith, G. R. Isaak, R. New, M. P. Ralls, and Z. P. van Zyl, J. Phys. B 12, L1 (1979).
[27]J. A. R. Griffith, G. R. Isaak, R. New, and M. P. Ralls, J. Phys. B 14, 2769 (1981).
[28]J. A. Nolen and J. P. Schiffer, Annu. Rev. Nucl. Sci. 19, 471 (1969).
[29]B. C. Carlson and G. L. Morley, J. Math. Phys. 3, 209 (1962).
[30]F. D. Becchetti, W. Makofske, and G. W. Greenlees, Nucl. Phys. A190, 437 (1972).
[31]N. Auerbach, J. Hüfner, A. K. Kerman, and C. M. Shakin, Rev. Mod. Phys. 44, 48 (1972).
[32]J. Jänecke, F. D. Becchetti, W. S. Gray, R. S. Tickle, and E. Sugarbaker, Nucl. Phys. (to be published).
[33]F. D. Becchetti, W. S. Gray, J. Jänecke, R. S. Tickle, and E. Sugarbaker, Nucl. Phys. A271, 77 (1976).
[34]J. H. Bjerregaard, O. Hansen, O. Nathan, and S. Hinds, Nucl. Phys. 86, 145 (1966); W. McCatchie, W. Carcey, and J. E. Kitching, *ibid.* A159, 615 (1970); P. Debenham and N. M. Hintz, *ibid.* A195, 385 (1972); D. G. Fleming, C. Gunther, G. Hageman, B. Herskind, and P. O. Tjøm, Phys. Rev. C 8, 806 (1973); W. Oelert, G. Lindstrom, and V. Riech, Nucl. Phys. A233, 237 (1974); A. Saha, O. Scholten, D. C. J. M. Hageman, and H. T. Fortune, Phys. Lett. 85B, 215 (1979).
[35]P. H. Stelson and L. Grodzins, Nucl. Data Tables A1, 21 (1965); S. Raman, W. T. Milner, C. W. Nestor, and P. H. Stelson, in *Proceedings Of The International Conference on Nuclear Structure, Tokyo, 1977,* edited by T. Marumori (Physical Society of Japan, Tokyo, 1978), p. 79.
[36]K. E. G. Löbner, M. Vetter, and V. Hönig, At. Data Nucl. Data Tables A7, 495 (1970).
[37]J. Jänecke, Phys. Lett. B103, 1 (1981).
[38]W. J. Tomlinson and H. H. Stroke, Nucl. Phys. 60, 614 (1964).
[39]B. S. Reehal and R. A. Sorensen, Nucl. Phys. A161, 385 (1971).
[40]W. D. Myers, Lawrence Berkeley Laboratory Report LBL-14310, 1982 (unpublished).
[41]Ch. Lagrange, J. Lachkar, G. Haout, R. E. Shamu, and M. T. McEllistrem, Nucl. Phys. A345, 193 (1980).
[42]H. Clement, R. Frick, G. Graw, F. Merz, H. J. Scheerer, P. Schiemenz, N. Seichert, and Sun Tsu Hsun, Phys. Rev. Lett. 48, 1082 (1982).
[43]O. Scholten, F. Iachello, and A. Arima, Ann. Phys. (N.Y.) 115, 325 (1978).
[44]O. Scholten, private communication.